Experimental and Numerical Studies on the Role of Dynamic Stress in Vibratory Stress Relieving Process

Duong Nguyen Van
Department of Materials Science and Engineering, Le Quy Don Technical University, Hanoi, Viet Nam
Email: duongdmse@gmail.com

Cuong Do Manh and Si Do Van
Department of Engineering Mechanics, Le Quy Don Technical University, Hanoi, Viet Nam
Email: bmanhcuongkck@gmail.com, vansihvkt@gmail.com

***Abstract*—This work aims to measure the dynamic stress in specimens during vibration treatment and to judge its relation with the relaxation of residual stress. Specimens with residual stress were vibrated at natural frequency on a dynamic shaker with different accelerations (different applied loads). Dynamic stress was calculated from dynamic strain that was measured with a strain gauge on the specimen surface. Residual stress in the specimens before and after vibratory stress relief was measured by hole drilling method. Finite element analysis for the specimens was performed at natural frequency with various applied loads. Results from experiments and simulation have shown a nonmonotonous dependence of residual stress reduction on applied load although dynamic stress monotonously increases as applied load increases. Stress reduction effectiveness increases as applied load increases due to dynamic stress increasing, but when the applied load exceeds some value stress reduction effectiveness decreases with increasing applied load.**

***Index Terms*—residual stress, dynamic stress, vibratory stress relief, cyclic load, finite element analysis**

I. Introduction

Many technological processes such as welding, casting,… produce residual stresses. These stresses often have bad effects on the work piece: decreasing the load capacity, increasing corrosion attack, increasing dimension instability and decreasing the manufacturing precision [1]. Many work pieces undergo stress relieving treatment after mechanical treatment to improve dimension stability or increase service life. Traditionally, work pieces are thermally treated by putting them in the furnace at high temperature for a certain length of time followed by slow cooling to room temperature. At elevated temperature the yield limit of materials become lower than the residual stress in the work piece, so the plastic deformation takes place and leads to reduction of residual stress. The thermal method of stress relief is effective but it also has some disadvantages: high cost due to high energy consumption, size limitation of treated work piece due to the size of the furnaces, oxidation and scaling of the work piece [2-3].

Some decades to now, vibratory stress relief (VSR) is considered as an alternative method to thermal treatment in stress relieving of work pieces. The VSR process can be described as follows: a stimulator is clamped to work piece and vibrates it; Frequency of the stimulator is adjusted to the resonant frequency of the work piece and this resonant vibration is maintained for a predetermined length of time for stress relieving to take place [4]. The method of VSR has overcome the mentioned disadvantages of thermal stress relief. This technology has been applied successfully in manufacturing of large steel work pieces such as: welded shaft, marine shaft, large rail [5-7]. VSR technology was also extended to work pieces by materials other than steel: large surface plate from stainless steel, thin parts from aluminum alloy [8-9].

Application of VSR technology in production was based on studying effect of vibrating parameters on the stress reduction. Most of researchers suggested that the treatment should be carried out at natural frequency of the work piece to bring it to resonant state with enough amount of deformation strain [10, 11]. The time of vibration at resonance may vary to an extend of 10 minutes or less. Amplitude of the applied load is another significant parameter, but there is no concrete range in choosing this. According to different authors, load amplitude must be sufficient to induce microscopic plastic deformation to bring about stress relaxation [3, 12]. But the way the applied load amplitude affects the stress reduction result is not really clear.

Effects of vibrating amplitude on the results of VSR are directly related to its stress relaxation mechanism, however, there are few studies on this fundamental aspect of the technology. From experiments with steel specimens, a hypothesis on the plastic deformation of stress reduction was proposed [13,14]. Recently, in Hanjun Gao's work [15], VSR was conducted on specimens from 7075 aluminum alloy. The result for aluminum alloy was similar to results for steels and

Manuscript received March 1, 2022; revised July 29, 2022.

© 2022 Int. J. Mech. Eng. Rob. Res

doi: 10.18178/ijmerr.11.9.690-697

suggested the relation between plastic deformation and stress reduction in VSR.

Effects of technological parameters on vibratory stress relief have also been simulated numerically [16, 17]. These simulations have fairly well demonstrated effects of vibration frequency and vibration time on stress reduction. S. Kwofie [18] established an equation describing the mechanical behavior of materials with residual stress under cyclic load. This gave stress–strain characteristics, stress-relaxation curve similar to those observed experimentally.

The mechanism of VSR can be addressed in a broader context as the residual stress relaxation under cyclic load. C. H. Lee et al. [19-20] showed stress relieving can occur after a few cycles of loading and the stress reduction depends on the amplitude of the cyclic load. Different material model have been used to predict the residual stress relaxation in welded aluminum plates [21] or in hot-rolled sheet steel [22]. Experiments have been conducted to verify the simulation results and shown a good agreement between experiment and simulation for the initial loading cycles.

Many authors in literature have suggested that the applied load in VSR should be high enough to cause residual stress reduction, but the further effect of applied load on stress reduction has not been surveyed. Moreover, stresses present in the specimens during VSR process include: residual stress and dynamic stress that is caused by cyclic external load during VSR. These stresses should be measured and calculated to access the effect on the stress reduction. In this study, an attempt was made to measure the dynamic stress in the specimen during VSR process. This was conducted by measuring the dynamic strain generated in in specimen upon vibration. Then the total stress in specimen was calculated to judge the role of dynamic stress in residual stress reduction. In addition, previous simulations on VSR only guessed bit did not reveal the plastic deformation upon stress relaxation process. In this study, a program on ANSYS was coded to monitor the plastic deformation in specimen and to relate this with the stress relaxation process.

II. Material and Methods

Experiments on VSR of steel specimens were carried on a dynamic shaker V830-335 of LDS Test and Measurement, UK. Specimens for experiments are steel plates having a rectangular base with four holes to clamp it to the dynamic shaker and a long body with a hole to attach the accelerator (Fig. 1). The specimens with thickness of 6 mm were made from ASTM A36 steel. Mechanical properties of the steel plates, obtained by tensile test, are as follows: σ_u = 440 MPa; σ_y = 290 MPa; δ = 17%.

Residual stress in each specimen was generated by thermal method. The specimens were locally heated at transition area between the body and the base parts by an oxyacetylene torch running along the heating line (Fig. 1). The heating process is displayed in Fig. 2a. Distance between the torch and the specimen, speed of the torch's movement were kept so that the heating zone has a width of 6mm and the temperature is about 1000 ^{0}C. After heating, the specimens were quickly cooled in water to obtain the high residual stress at the transition area. According to the shape of the specimens and the scheme of vibrating test (in next paragraph), this area is also expected to have the highest value of dynamic stress during the test.

Specimens were clamped to the vibrating table of V830-335 dynamic shaker with four bolts at the base part. As the vibrating table moves vertically with a specific acceleration, different parts of the specimen will undergo different displacements, therefore its body will be deformed during the test. Deformation during vibration treatment may cause the reduction of residual stress in the specimens. With this LDS shaker, beside vibrating frequency it is possible to adjust the acceleration of vibration. In principle, each vibrating frequency of the table is equivalent to a certain load applied on the specimen.

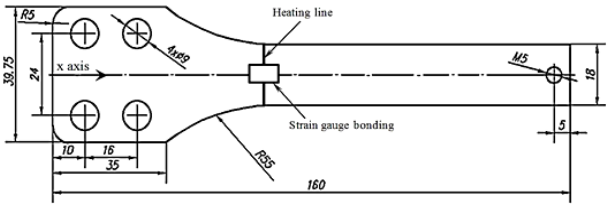

Figure 1. Dimensions of test specimens.

a)

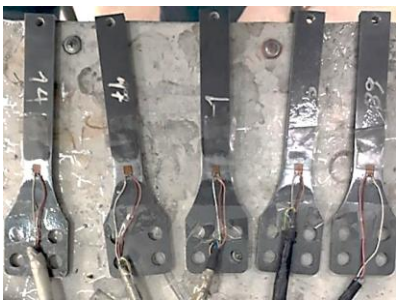

b)

Figure 2. Heating of the specimens to generate residual stress (a) and strain gauge FLA-5-11 for measuring strain during vibration treatment (b).

Specimens were clamped to the vibrating table of V830-335 dynamic shaker with four bolts at the base part. As the vibrating table moves vertically with a specific acceleration, different parts of the specimen will undergo different displacements, therefore its body will be deformed during the test. Deformation during vibration treatment may cause the reduction of residual stress in the specimens. With this LDS shaker, beside vibrating frequency it is possible to adjust the acceleration of vibration. In principle, each vibrating frequency of the table is equivalent to a certain load applied on the specimen.

III. Experiments Material

A group of 5 specimens have been prepared and for each of them a strain gauge FLA-5-11 of Tokyo Sokki Kenkyujo was attached to its transition zone where the residual stress has highest value (Fig. 2b). The strain gauge at the position as in Fig. 1 was aligned to monitor the strain along the x-direction in this figure, that is the main direction of the specimen. With the use of accelerators as shown in Fig. 3, natural frequency of specimens was found to be of around 283.5 Hz. Each of the 5 specimens was vibrated on the table at natural frequency, 283.5 Hz, with different accelerations: a = 10-200 m/s2. The strains during each resonant test were collected with LMS data collector, then amplitudes of strain oscillations were calculated. Each obtained strain was the mean value of the 5 strain amplitudes from 5 specimens.

Eight specimens with residual stress at the transition zone in the range of 205-230 MPa were used for the vibratory stress relief experiment. Each specimen was vibrated on the vibrating table at resonant frequency, 283.5 Hz, for 10 minutes with a specific acceleration to create a certain amount of dynamic stress on the specimen. Before and after VSR, residual stress at transition zone in each specimen was measured by hole drilling method according to ASTM E837-2008 standard [23].

The position of strain rosettes on specimens is the same as the position of strain gauges as shown in Fig. 2b and the rosettes were aligned so that direction of the first gauge coincide with the x-direction in this figure. Residual stress in specimen was calculated from the relaxed strains by a procedure described in ASTM E837-2008. For the ease of comparison of residual stress before and after vibratory stress relief, residual stress was computed according to the case of uniform stress.

Figure 3. Specimens with strain gauges on vibrating table of LDS dynamic shaker.

IV. Simulation

Modeling the VSR process is another approach to validate the hypothesis on the mechanism of stress relaxation. The simulation was carried out in ANSYS APDL package for the specimen with geometry shape and materials properties as specimens for experiment above Fig. 1. Harmonic analysis for this steel plate gave the first resonant frequency of 383,06 Hz. Further in the study, vibration for stress relieving was carried out at this resonant frequency.

In this study, the heat source for heating the specimen was taken as an arc-welding source which was a traveling two-dimensional source with Gaussian distribution. The heat flux distribution on the surface of the solid is related to the radial position r (whose origin is the arc center), as follows [24]:

$$Q(r) = U.I.\eta.\frac{k}{R^2}e^{(k.(x^2+(y-vt)^2)}. \quad (1)$$

where Q(r) is the surface flux at radius r, η is the efficiency coefficient, U is the voltage, I is the current and v is the travel velocity of the welding torch, x and y – surface coordinates of the welding torch. R, k - constants of the heat flux concentration.

Analysis of temperature distribution for welding was conducted with following parameters: U=20 V, I=160 A, v=3 mm/s, R = 0,006, k = 1/3, η = 0,85. The total time for heating and cooling was 1100 s. The temperature distributions in the specimen at various time was calculated and recorded.

The residual stress and quenching deformation are calculated from the thermo-mechanical properties of A36 steel and temperature distribution. In this modeling the specimen is assumed to be clamp at one edge of base part. Materials model for thermo-mechanical problem is bilinear kinematic hardening [25]. Temperature dependence of the materials constants were taken as those of an equivalent steel grade, CT3 steel GOST 2590-88, from literature [26].

Specimen with residual stress, as in Fig. 1 clamped at the end of base part, is subjected to a external cyclic load at the end of the steel plate. This is a surface load put on the inner of the M5 hole in the head of specimen (see Fig. 1). The frequency of cyclic load is chosen to be resonant frequency of 383,06 Hz and time of vibration is equivalent to 60 load cycles. Therefore, applied load on the specimen varies with time:

$$F_{app} = A.\sin(2\pi ft). \quad (2)$$

where A –amplitude of applied load; f – frequency of the cyclic load, f = 383.06 Hz; t – time at vibration treatment. Different cyclic load's amplitudes were chosen for simulation: 5N, 10N, 20N, 30N, 40N, 50N, 55N. After each run at a specific amplitude specimen was brought to unloaded state by being additionally vibrated at zero amplitude (A=0) for 20 cycles. This was called "die-out" time to stabilize the stress state in the specimens.

V. Results and Discussions

Fig. 4 represents the dynamic strains at different vibration amplitudes at the strain gauge position during VSR of the specimen. Dynamic strain in this case is the amplitude of oscillating strain generated by specific acceleration amplitudes applied to the specimen. As it is

© 2022 Int. J. Mech. Eng. Rob. Res

well known, this acceleration amplitude is proportional to the applied load's amplitude. It is obvious from this experiment that dynamic strain was not simply proportional to the acceleration (or applied load) for these specimens vibrating at resonance. To the first approximation, relation between dynamic strain and vibrating acceleration of the specimen could be fitted by formula:

$$\varepsilon = 216.222 * (\frac{a}{g})^{0.783}. \quad (3)$$

With ε – strain at the transition zone, x10^{-6};
a – acceleration, m/s^2;
g – gravity acceleration, g = 10 m/s^2.

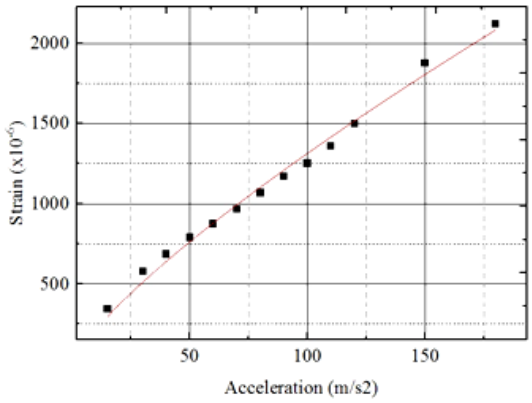

Figure 4. Experimental relationship between test acceleration and strain at transition zone for specimen at resonant vibration.

According to scheme of strain gauge bonding, the obtained dynamic strain was amplitude of strain along the x direction of specimens. Therefore, dynamic stress (amplitude of dynamic stress) along the x-direction at the position of strain gauge could be calculated:

$$\sigma_{dy} = E.\varepsilon_{dy}. \quad (4)$$

Where: σ_{dy} - dynamic stress along the x direction at the position of strain gage;

ε_{dy} – dynamic strain along the x-direction at the position of strain gauge;

E - elastic modulus of the specimen's materials, E = 210 GPa.

Table I shows the vibration accelerations for specimen and the dynamic strain along x direction at the strain gauge positions on the specimens, obtained from formula (3) or Fig. 4. Also in the table: σ_{0x}, σ_{1x} are the stresses along the x-direction before and after VSR, respectively; σ_{dy} is the dynamic stress along x-direction caused by vibrating table at the strain gauge position, calculated from formula (4); σ_{tx} is the total stress a long x-direction at the gauge's position caused by residual stress and dynamic stress along the x direction: $\sigma_{tx} = \sigma_{0x} + \sigma_{dy}$; R is effectiveness of residual stress reduction, estimated by the reduction in the x-direction stress [13, 15, 16]:

$$R = (\sigma^0_x - \sigma^1_x)/\sigma^0_x.100\% . \quad (5)$$

TABLE I. RESIDUAL STRESS IN SPECIMENS AFTER VIBRATORY STRESS RELIEF

Specimen	N1	N2	N3	N4	N5	N6	N7
a, (m/s^2)	15	30	40	55	70	100	170
ε_{dy} (x10^{-6})	345	580	686	859	967	1252	1890
σ^0_x, Mpa	205	213	220	206	210	215	214
σ^1_x, Mpa	190	129	118	39	64	99	112
σ_{dy}, Mpa	69	116	137	170	193	250	381
σ_{tx}, Mpa	274	329	357	376	403	465	595
R, %	7,3	39,4	46,4	81	69,5	54	47,6

As indicated in Table I, vibration with small acceleration, around 15 m/s2 in specimen N1, caused a dynamic stress in the x-direction of 68 MPa. This dynamic stress grew up to hundreds of megapascals as vibration acceleration increased (specimens N2-7). But for low vibrating acceleration (specimen N1) the dynamic stress at the strain gauge position was not high enough and the total stress along the x direction (274 MPa) was below the yield limit of this materials (290 MPa). Therefore, its residual stress reduction was very low (only 7,3%).

As the vibrating acceleration increased in specimens N2-4 the dynamic stress gradually increases to 116, 137, 170 MPa. Consequently, residual stress decreased and stress reduction effectiveness grew up. This can be explained by the fact that the total stress along x-direction for these specimens was visibly higher than the yield limit of the materials. The good results have been obtained with specimens N4 where the stress reduction effectiveness can reach to 81%. But as the vibration acceleration increased further in specimens N5, N6, N7, the stress reduction effectiveness fell to lower values, only 46,7% for specimen N7 (Fig. 5). At the same time the total stress along x direction in these specimens far exceeded the materials' yield limit, e.g. 570 MPa for specimen N7.

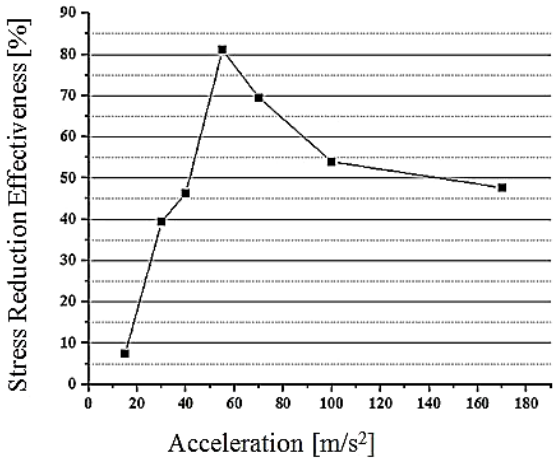

Figure 5. Stress reduction effectiveness of VSR at different accelerations.

It is clearly shown in this experiment that stress reduction of vibration treatment effect appeared clearly when the dynamic tress was high enough, and therefore

applied load must be high enough to sum up with the existing residual stress. However, if the vibration acceleration was too high, and the dynamic stress gets to very high value. As a consequence, the specimen is heavily deformed with large difference in the amount of plastic deformation between various parts of the specimen. Therefore, after unloading additional residual stress will be created and resulting residual stress grows up to higher value, effectiveness of VSR process will decrease (Fig. 5). This has a practical meaning that applied load on one hand should be high enough to bring about the stress reduction effect. On the other hand this load should not be too high, otherwise VSR can take the work piece to a state of heavy plastic deformation and cause additional residual stresses, therefore effectiveness of VSR will be low. In addition, very high load can be less cost-effective as it will require more energy and cause difficulties for implementing the vibration scheme.

The obtained corelation of stress reduction effectiveness with the total stress in specimens may suggest the occurenece of plastic deformation during stress relaxation process. Nevertheless, it is unfeasible to express the plastic deformation condition for residual stress relaxation as in literature [13-15]. The reason is that as total stress was lower than materials yield limit in specimen N1, the stress reduction efffect was still existent at low value (7.3%).

Simulation provided additional confirmation to the experimental results. Distribution of x-direction stress and first principal stress along the heating line in specimen before VSR are shown in Fig. 6. As is shown by the data in the figures, along the heating line the first principal stress (maximum stress) did not coincide with the x-direction stress (direction perpendicular to the heating line). This meant the angle between first principal stress and heating line was slightly different from 90 degrees. In addition, the x-direction stress and first principal stress got to maximum near the center of the heating line (postion in the distance 9 mm). These may be due to the narrow width of the specimen, and the heating line (18 mm). Moreover, the position of stress maxima was also the position of strain gauge for dynamic stress measurement and residual stress measurement in the experiment. Also, this position was expected to be where the stress reduction would be most likely to occur with high effectiveness during VSR.

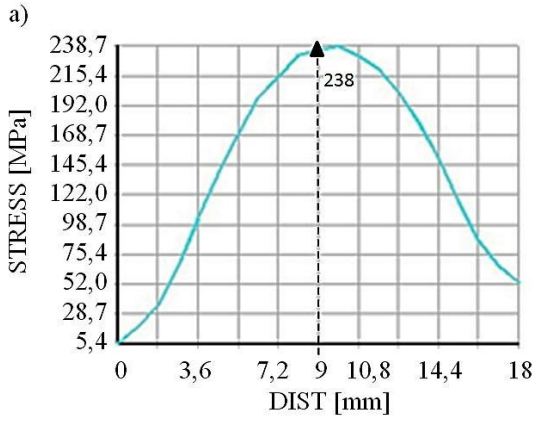

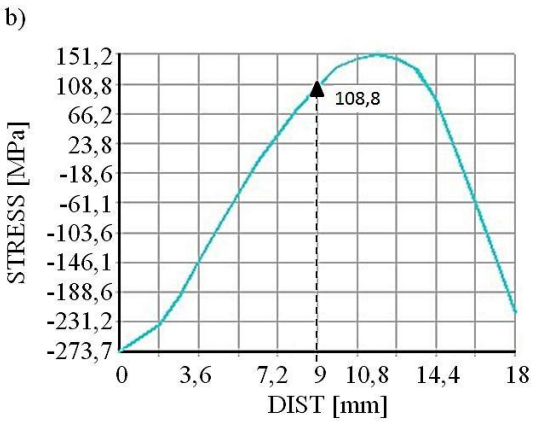

Figure 6. Distribution of X-direction stress (a) and first principal stress (b) along the heating line in the specimen after heating and cooling.

Fig. 7 represents residual stress in the specimens after vibration treatment at resonant frequency and 60 cycles with various applied load's amplitude. At the load with low amplitude, 3N or 5 N, there happened residual stress reduction in specimen with very low effectiveness. When the load increased to 20 N, 30 N, the dynamic stress certainly also raised. Therefore, the residual stress declined obviously: maximum of x-direction stress was reduced from the initial value of 151,2 Mpa in Fig. 6a to the maximum of 8,7 MPa after treatment with a 30 N applied load in Fig. 8.

But as the amplitude of external force grew further, to 55 N for example, the residual stress went up even to the value higher than initial value (218 MPa in Fig. 9). This meant stress reduction effectiveness declined. Furthermore, in comparison with Fig. 6 and Fig. 8, Fig. 9 shows a quite different distribution of residual stress along the heating line after VSR at 55 N. This can be explained that high applied load has brought the specimen to the state of heavy plastic deformation as explained with the aforementioned experiment. Therefore, additional residual stress has been created and residual stress along the heating line changed drastically.

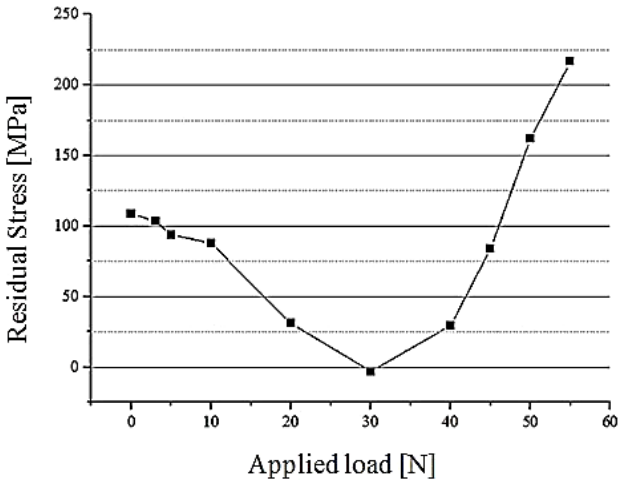

Figure 7. X-direction stress at center of heating line after VSR at resonant frequency with different applied loads.

© 2022 Int. J. Mech. Eng. Rob. Res

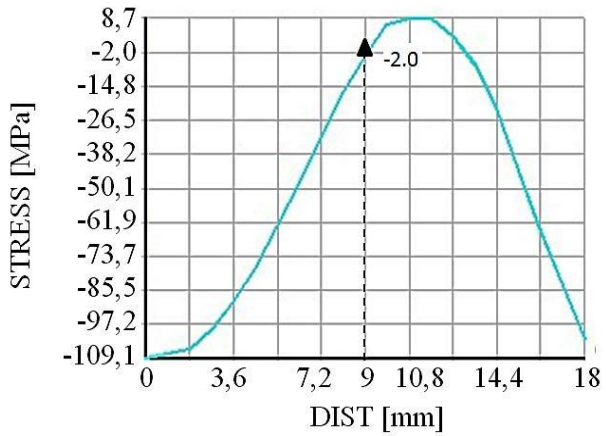

Figure 8. Distribution of x-direction stress along the heating line after VSR with applied load of 30N

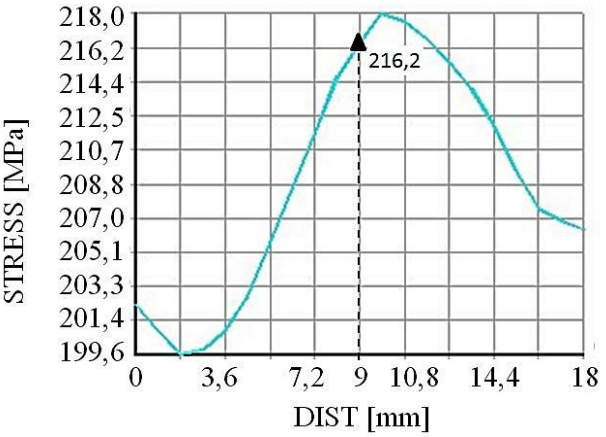

Figure 9. Distribution of x-direction stress along the heating line after VSR with applied load of 55N.

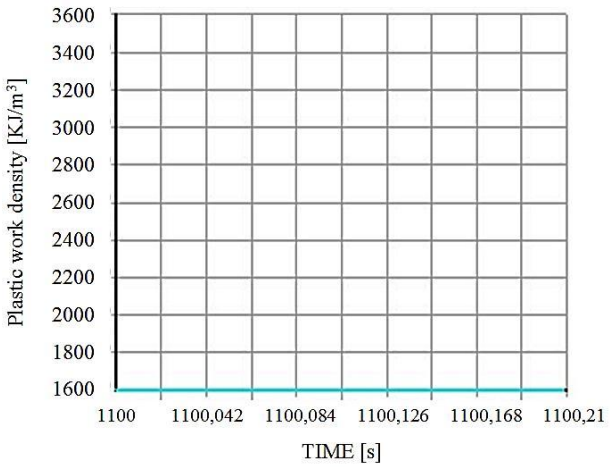

Figure 10. Change in plastic work density at node 412 during VSR process with applied load of 5 N.

Fig 10-11 show changes of plastic work density at node 412 vs. time of vibration with different load amplitudes. Node 412 lies on the surface of the specimen at the center of the heating line, and this was also the position of strain gauge for residual stress measurement in the experiment. At a low external load of 5 N, the plastic deformation did not occur as plastic density did not change (Fig. 10), therefore change in residual stress of the specimen was very small. At higher load with amplitude of 20 N this node endured plastic deformation (Fig. 11), residual stress in the specimen reduced drastically (Fig. 8). Indications of plastic deformation have been also obtained in simulations at 30 N, 45 N, 50 N, 55 N applied loads with higher plastic work density (not shown by figures). These showed a correlation between the micro plastic deformation and stress relaxation upon VSR process in this simulation.

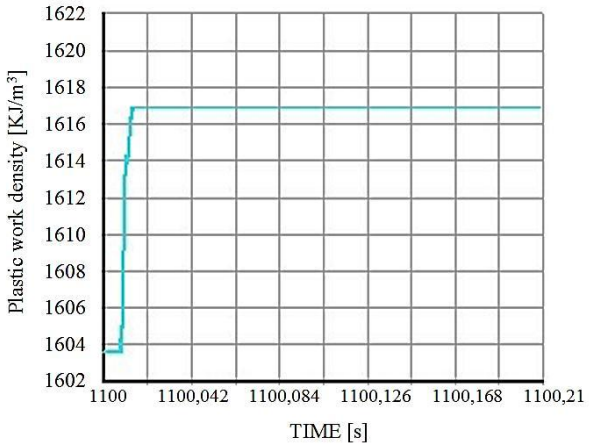

Figure 11. Change in plastic work density at node 412 during VSR process with applied load of 20N.

Moreover, it is worth noting that with the materials model of bilinnar kinematic hardending, criteria for plastic deformation is value of equivalent stress. But this equivalent stress is not additive, it means equivalent stress of the total state at a point is not the sum of equivalent stress of residual stress and equivalent stress of dynamic stress. Hence, it is not possible to state about the relation between total of residual stress and dynamic stress with the yield limit of materials. Therefore, the interaction between dynamic stress and residual stress should be investigated and different hardening models need to be taken into account upon simulation of VSR process.

VI. Conclusions

In this study, steel plates were vibrated at resonant frequency on a dynamic shaker at different accelerations. The residual stress before and after vibration treatment, and dynamic strain during vibration were measured. Simulation of the vibration treatment for specimen was also conducted with different applied load amplitudes with bilinear kinematic hardening model. Stress state, plastic work density in critical point of in the specimen after vibration were observed. Several conclusions can be drawn as follows:

- As the applied load's amplitude increased the dynamic stress in specimen increased monotonously. The dynamic stress could reach very high value, several hundreds of MPas, to add to existing residual stress.
- As the dynamic stress increased due to increasing of applied load, the residual stress reduced and residual stress effectiveness could get to 81% at

vibration acceleration of 55 m/s2. But as applied load, and dynamic stress, exceeded certain values, the residual stress increased again and stress reduction effectiveness reduced. This non-monotonous dependence of the residual stress was explained by the arrival of specimens to a heavy deformation state and, consequently, additional residual stress had been produced.

- Simulation at resonance with different load amplitudes also demonstrated the nonmonotonous dependence of residual stress reduction on applied load. The simulation point out that the residual stress reduced obviously only when the dynamic stress was high enough to cause micro plastic deformation in specimens.

Further studies need to be carried out to investigate the way that dynamic stress combines with residual stress to reduce the latter and to investigate the effect of plasticity behavior of the material on the stress relaxation process.

CONFLICT OF INTEREST

The authors declare no conflict of interest.

AUTHOR CONTRIBUTIONS

Conceptualization of the work was proposed by Duong Nguyen Van; Methodology for this was presented by Cuong Bui Manh; Si Do Van and Cuong Bui Manh conducted the experiments; Simulation was performed by Si Do Van, Duong Nguyen Van; Writing was completed by Duong Nguyen Van and Si Do Van.

REFERENCES

[1] S. Chen, Y. Zhang, Q. Wu, H. Ago, and D. Yan, "Residual stress relief for 2219 aluminum alloy weldments: A comparative study on three stress relief methods," *Metals*, vol. 9, no. 419, 2019.

[2] A. Fayrushin, "The effects of vibration treatment in the process of welding on the structure of metal of seam weld," *IOP Conf. Series: Earth and Environmental Science*, vol. 459, no. 062110, 2020.

[3] M. Patil, R. Rohidas, D. Sarode, "Vibratory residual stress relief in manufacturing–a review," *International Journal of Engineering and Sciences & Research Technology*, vol. 6, no. 5, pp. 609-613.

[4] G. Cai, Y. Huang, I. Huang, "Operating principal of vibratory stress relief device using coupled lateral-torsional resonance," *International Journal of Vibroengineering*, vol. 19, no. 6, pp. 4083-4097, 2017.

[5] A. Munsi, A. Waddell, C. Walker, "Vibration stress relief–an investigation of the Torsional stress effect in welded shafts," *Journal of Strain Analysis*, vol. 36, no. 5, pp. 453-464.

[6] M. Sun, Y. Sun, and R. Wang, "The vibratory stress relief of a marine shafting of 35# bar steel," *Materials Letters*, vol. 58, no. 3, pp. 299–303, 2004.

[7] D. Rao, J. Ge, and L. Chen, "Vibratory stress relief in manufacturing the rails of a Maglev system," *Journal of Manufacturing Science and Engineering*, vol. 126, no. 2, pp. 388-391, 2004.

[8] D. Rao, D. Wang, L. Chen, and C. Ni, "The effectiveness evaluation of 314L stainless steel vibratory stress relief by dynamic stress," *International Journal of Fatigue*, vol. 29, no. 1, pp. 192–196.

[9] H. Gong, et al. "Effect of vibration stress relief on the shape stability of aluminum alloy 7075 thin-walled parts," *Metals*, vol. 9, no. 27, 2019.

[10] A. Hassan, "Fundamentals of vibratory stress relief," *Asian Journal of Applied Science*, vol. 7, no. 5, p. 317-234, 2014.

[11] M. Selemenev, "Increasing the efficiency of vibration treatment of complex surfaces," *IOP Conf. Series: Materials Science and Engineering*, vol. 709, no. 044077, 2020.

[12] C. Walker, "A theoretical review of the operation of vibratory stress relief with particular reference to the stabilization of large-scale fabrications," in *Proc. IMechE, part L: J. Materials: Design and Applications*, vol. 225, no. 3, p. 195-204, 2011.

[13] C. Walker, A. Waddell, and D. Johnston, "Vibratory stress relief – an investigation of underlying process," in *Proc. the Institution of Mechanical Engineers, Part E: Journal of Process Mechanical Engineering*, vol. 209, no. 1, p. 51-58, 1995.

[14] Z. Qian, S. Chumbley, T. Karakulak, and E. Johnson, "The residual stress relaxation behavior of weldments during cyclic loading," *Metallurgical and Materials Transactions A*, vol. 44, p. 3147–3156, 2013.

[15] H. Gao, et al. "Experimental and simulation investigation on thermal-vibratory stress relief process for 7075 aluminum alloy," *Materials & Design*, vol. 195, no. 12, p. 108954, 2020.

[16] X. Zhao, Y. Zhang, H. Zhang, Q. Wu, "Simulation of vibration stress relief after welding based on FEM," *Acta Metallica Sinca (English Letter)*, vol. 21 no. 4, pp. 289-294, 2008.

[17] Y. Yang, "Understanding of vibration stress relief with computation modeling," *Journal of Materials Engineering and Performance*, vol. 18, no. 7, p. 856–862, 2009.

[18] S. Kwofie, "Plasticity model for simulation, description and evaluation of vibratory stress relief," *Materials Science and Engineering A*, vol. 516, no. 1-2, p. 154–161, 2009.

[19] J. Cho, C. Lee, "FE analysis of residual stress relaxation in a girth-welded duplex stainless steel pipe under cyclic loading," *International Journal of Fatigue*, vol. 82, pp. 462–473, 2016.

[20] C. Lee, K. Chang, and N. Vuong, "Finite element modeling of residual stress relaxation in steel butt welds under cyclic loading," *Engineering Structures*, vol. 103, pp. 63-71, 2015.

[21] Y. Dehkordi, A. Anaraki, A. Shahani, "Comparative study of the effective parameters on residual stress relaxation in welded aluminum plates under cyclic loading," *Mechanics & Industry*, vol. 21, no. 505, 2020.

[22] P. Zobec, J. Klemenc, "Application of a nonlinear kinematic-isotropic material model for the prediction of residual stress relaxation under a cyclic load," *International of Fatigue*, vol. 150, no. 106290, 2021.

[23] ASTM E837-08 (2008). Standard Test Method for Determining Residual Stresses by the Hole-Drilling Strain-Gage Method. ASTM International, West Conshohocken, PA. Doi: 10.1520/E0837-08.

[24] J. Goldak, A. Chakravarti, and M. Bibby, "A new finite element model for heat sources," *Metallurgical Transactions B*, vol. 15B, pp. 299-305, 1986.

[25] ANSYS (2013), *ANSYS ADPL element reference -Release 13.0*, ANSYS, Inc., Pennsylvania, p. 22-30.

[26] B. G. Sorokina, M. A. Garvacieva, *Steel Grades*, *Intermet Engineering*, *Moscow*, pp. 574-578. (Russian language), 2001.

Copyright © 2022 by the authors. This is an open access article distributed under the Creative Commons Attribution License (CC BY-NC-ND 4.0), which permits use, distribution and reproduction in any medium, provided that the article is properly cited, the use is non-commercial and no modifications or adaptations are made.

Duong Nguyen Van was born on June 7th 1976 in Nam Dinh, Vietnam. Duong Nguyen Van graduated form Le Quy Don Technical University with a degree of engineer in materials engineering. In 2006, Duong Nguyen Van received PhD degree in materials science in Moscow Institute of steel and alloys. He is now head at department of materials and engineering, Le Quy Don Technical University. His research interests include metal heat treating, residual stress in metallic materials, magnetic materials. He has conducted 4 research projects and published more than 30 papers. Dr. Nguyen is member of Vietnam Association of Heat Treating Science and Technology. Dr. Nguyen has won second prize in Vietnam Science & Technology Innovation Awards 2020.

Cuong Bui Manh was born on January 27, 1980 in Việt Nam. Cuong Bui Manh graduated from Le Quy Don Technical University in 2004, and received Ph.D. degree in engineering mechanics at Irkutsk National Research Technical University, Irkutsk, Russia in 2011. He is Head of Department of machinery design, Le Quy Don Technical University, Hanoi, Vietnam. His scientific direction - fatigue life of machines, optimal design of machines and machine parts under fatigue life, fracture mechanics. He has conducted fourteen research projects related to numerical methods for the simulation of endurance, fatigue life and technological processes. In addition, Dr. Bui has published 30 papers in qualified journals and conferences. Dr. Bui is member of Vietnam Association of Mechanics. Dr. Bui has won second prize in Vietnam Science & Technology Innovation Awards 2020. Dr. Bui also won the First Prize for PhD student of outstanding performance (2008) at Irkutsk National Research Technical University, Irkutsk, Russia.

Si Do Van was born on January 10, 1981 in Việt Nam. He received the BS, MS degrees in Mechanical Engineering from Le Quy Don Technical University, Ha Noi, Viet Nam in 2006 and 2012. Respectively, He is currently a PhD student at Le Quy Don Technical University, Ha Noi, Viet Nam. His research interests include development of mathematical models and numerical methods for analysis of the dynamics and strength of machines, optimal design of machines and machine parts under fatigue life.

© 2022 Int. J. Mech. Eng. Rob. Res